Deliverable

5.2. Upscaled scenarios and uncertainties at broader scale

Tobias Conradt

Potsdam-Institute for Climate Impact Research
Telegrafenberg, Potsdam, Germany

Finalized in May 2023

Contents

0 Background and adjusted scope of this deliverable

The title of this deliverable could be abbreviated to “Drought scenarios at broader scale”, and the original idea was probably to provide a modelling-supported upscaling of drought impact scenarios from the regional case studies to the European continent. We have to admit that this aim was set too high. The eco-hydrological model SWIM developed at PIK (Krysanova et al. 1998) which has a long history of successful applications in large river basins around the world (Krysanova et al. 2015) was planned to be applied to all of Europe, but the complexity of this task was under-estimated. Additional retarding factors were a general overhaul of the original Fortran code which had seen many amendments by different programmers with different coding styles. The re-write altered many data formats and interfaces and additionally introduced the Python programming language for pre- and postprocessing. Albeit reproducible modelling was not guaranteed any more with the old code and the overhaul was therefore inevitable, it required new ways of operation which could not be easily acquired by the team. The chief developer responsible for this transition left PIK in 2021 when there were still many open issues, and the hydrologist tasked with setting up SWIM Europe also went to another employer one year later. At the time of writing, the continental SWIM setup is still a construction site.

What we learned from the case studies was how differently the individual drought situations developed, beginning from different meteorological backgrounds (since drought is always relative to the local climate normals) to region-specific impact chains or non-impacts (e.g. a rural area depending on irrigation vs a lignite mining region with no lack of draining water for cooling their power stations). We therefore first took a step back and looked at the already existing drought scenarios for or including the European continent which are however often limited to the meteorological drivers. The main part of this deliverable is therefore devoted to researching the link between meteorological and soil drought across Europe – even without eco-hydrological modelling – as soil drought is the leading component in the drought cascade directly affecting vegetation growth including crop yields and, with a time lag of 2–3 years, forest health. Being able to calculate realistic root zone soil moisture distributions from meteorological variables on the large scale would be an important step in establishing reliable continental impact scenarios. As we will demonstrate, there are still significant deficits in root soil moisture modelling on these scales which may also question the validity of earth system or global circulation models including a land component.

1 The current state of drought scenarios for Europe

Drought risk is increasing in many parts of the world due to ongoing climate change (Caretta et al. 2022). For a detailed view into future trajectories in hydrological storages and vegetation, i.e. diminishing soil water contents in a certain agricultural region, projections of spatially distributed (eco-)hydrological models are needed, but these are still not widely available or reliable on the large scale.

Zhao and Dai (2022) presented an assessment of drought trends in the CMIP6 model ensemble considering 25 global circulation models (GCMs). The global change patterns for precipitation (P), evapotranspiration (ET), soil moisture (SM), and runoff (R) are quite similar to those observed in CMIP5-based studies; both P and ET are increasing in large parts of the world. In Europe, there are negative trends especially for P in the Mediterranean region, and the decreasing water balances show negative trends in SM, pronounced in the top layer over all of Europe, but also in the root zone with Scandinavia and the Baltic coast being the only exceptions. This is mirrored in R which is projected to decrease by 20% and more in southern Europe at the end of the 21st century under SSP5-8.5 conditions. Joo et al. (2020) warned also of earlier and stronger soil moisture depletion using statistically downscaled CMIP5 data.

The self-calibrating Palmer drought severity index (Palmer 1965, Wells et al. 2004, Dai 2011) was also calculated and analyzed for the CMIP6 scenarios by Zhao and Dai (2022). Already under SSP2-4.5 conditions this index is expected to decrease on average by 0.5–1.5 units in Central and Southern Europe towards the end of the 21st century, and under SSP5-8.5 the decreases exceed 2 units. In both scenarios, decreases are also possible in parts of Scandinavia, especially Finland. Given the fact that the index should fluctuate around zero under normal conditions and that a value below −3 is considered a severe drought, a general decrease by 2 units means severe droughts becoming a rather common phenomenon in most of Europe. Higher probabilities for hydroclimatic extremes can also be assumed from the observation of flattening probability distribution functions, i.e. an increasing variability. For agroclimatic droughts Zhao and Dai (2022) report increasing frequencies for most parts of the world with pronounced effects over Europe. Finally it must be noted that compared to the respective analysis of CMIP5 models under a RCP 4.5 scenario (Zhao and Dai 2015) the CMIP6 drought trend seems less concentrated over Southern Europe.

An earlier analysis of CMIP6 outputs regarding drought effects had been presented by Cook et al. (2020), however based on 13 GCMs only. Their soil moisture maps show the strongest decreasing trends not only over Southern Europe but also in Northern Scandinavia, especially during the northern hemisphere summer. The same spatial pattern is shown for the

occurrence probability increase for extreme droughts, but top-layer soil moisture is projected to decrase also over Central Europe.

These and other recent drought scenario assessments were critically highlighted in a CROSSDRO publication by Vicente-Serrano et al. (2022). Starting from global drought trend assessments of the recent past and being confronted with large discrepancies between trend maps of different drought indicators – depending on precipitation, evapotranspiration, or atmospheric evaporative demand (AED) being the principal variable – the authors conclude that these inconsistencies multiply with the notable uncertainties of global circulation models (GCM) so that the GCM-only based trend maps are generally questionable. Nevertheless, a clear signal towards increasing drought stress on vegetation caused by upward trends in AED could be identified for most world regions including Europe.

As already stated in the first paragraph of this section, the lack of soil moisture or runoff scenarios produced from global or continental hydrological models is striking. The hydrological scenarios cited by Vicente-Serrano et al. (2022) are extrapolations of statistical relationships to meteorological conditions (e.g. Dai 2021, Woodhouse et al. 2016, or Zeng et al. 2022). As we failed with our own attempt filling this gap (see previous section) we will now look at the connection between meteorological drought and some prominent root zone soil moisture reanalyses.

2 Connecting meteorological and soil drought

2.1 Introduction

Meteorological and soil drought indices correlate quite well if the time lag of soil drought is somehow considered (cf. Ajaz et al. 2019). Barnard et al. (2021) assessed the connections between the Standardized Precipitation Evapotranspiration Index (SPEI, Vicente-Serrano et al. 2010, Beguería et al. 2014) on different scales and dynamically modelled soil water profiles at 866 sites in the Midwestern U.S. In general, the strongest correlations for depths below 20 cm were found for a SPEI integrating twelve months, but process-based modelling was recommended especially for end-of-winter situations and sowing date determination.

A more broadscale and indirect attempt to connect weather to soil moisture patterns across Europe – by the North Atlantic Oscillation (NAO), Arctic Oscillation (AO) and El Niño Southern Oscillation (ENSO) indices – was made by Almendra-Martín et al. (2022). The authors also used ERA5 and LISFLOOD soil moisture (SM) data as reference excluding large parts of Scandinavia, the Alps and other, mostly mountainous patches in which their SM series are not clearly correlated or even contradictory ($r < 0.5$). As we will see below, even the direct correlations between SPEI and these SM data are low in mountainous areas. Sutanto et al. (2020) who mapped compound drought hazards using LISFLOOD for soil drought and ERA5 for fire risk (meteorological drought) consequently found low compound risk for just the same regions. Connections between ENSO and global soil moisture were also researched within CMIP6 scenarios (Le and Bae 2022), but they were found to be weak and not present in Europe.

In situ soil moisture (SM) measurements which provide direct information about the root zone soil water content are relatively scarce especially in Central and Northern Europe (Dorigo et al. 2021) albeit there are recent initiatives to densify the network, e.g. by cosmic-ray sensors (Bogena et al. 2022). For obtaining soil moisture fields simple spatial interpolation of the point measurements would therefore not work, a lot of landscape heterogeneity between the stations including different orographic conditions, soil textures, and local precipitation events requires consideration of these factors, for example by eco-hydrological modelling. A review by Liu and Yang (2022) illustrates the state of the art in tackling the problem among which process-based modelling, assimilation of satellite and meteorological data, data fusion and deep learning are common approaches.

Here we will investigate the feasability for approximating the root zone soil moisture distribution over Europe more or less directly from a spectrum of SPEIs on different scales. The idea is to map the correlations between each SPEI and soil moisture indices (SMI) from major global or European soil moisture products and see whether high correlations can be found for every location from any of the SPEI scales. Consequently using indices

tackles the complications from annual soil moisture cycles and regional differences in soil water storage availability and average saturation. If a common geographical pattern of SPEI scales for relatively high optimal correlations can be found it would provide an easy approach for deriving large scale soil drought maps from weather or climate scenario data without the need for using dynamical models. In any case, this exercise opens an unconventional view on the connection between meteorological drought and soil moisture dynamics.

While SPEI histories can be calculated from any high-resolution climate reanalysis or gridded weather data – we chose E-OBS, probably the best observation-based grid product for Europe – the collection of soil moisture data from different sources requires some effort regarding homogenizing different grids and time scales. What options exist for soil moisture products?

Within Germany, the mesoscale hydrological model (mHM) of the Helmholtz Centre for Environmental Research (UFZ), Leipzig, provides soil moisture for their Drought Monitor (UFZ 2023). A recent evaluation confirmed the high correlation with observed soil moisture especially during drought phases (Boeing et al. 2022). The performance of the new 1.2 km resolution version was however only slightly enhanced compared to version 1, and we can therefore rely on the publicly available data with 4 km resolution as best reference for the region.

Beck et al. (2021) recently evaluated 18 global soil moisture products. Despite the limitation of the comparisons to 5 cm soil depth also for root-zone products to include satellite products this might be the most comprehensive quality ranking available at the time of writing. Interestingly, only two remote sensing products are among the top ten regarding the highest median correlations ($\tilde{r}$) with the in situ measurements, and all models with data assimilation can be found in the front half of the field. The top four positions with median correlations of 0.74–0.78 to in-situ measurements are variants of the Hydrologiska Byråns Vattenbilansavdelning (HBV) hydrological model (Bergström 1976, 1992, Seibert and Bergström 2022) contributed by the authors; these data are however only available upon request. Among the generally available products including root zone soil moisture, ERA5-Land is the next-best ($\tilde{r} = 0.72$) followed by GLEAM ($\tilde{r} = 0.71$) and ERA5 with data assimilation ($\tilde{r} = 0.68$); GLDAS-Noah performs worst ($\tilde{r} = 0.60$) – this is in agreement with Li et al. (2021) who also observed strong biases in Noah-MP results. Anyway, these are the “big names” for large-scale soil moisture data. ERA-Interim, ERA5, and GLDAS served as basis for the evaluation of SM in CMIP6 Simulation by Qiao et al. (2022).

Accordingly, we considered ERA5, the fifth generation of European ReAnalysis, more precisely its ERA5-Land component (Muñoz-Sabater et al. 2021). Soil moisture is included and computed hourly by the ECMWF land model CHTESSEL which considers six different soil texture classes in the

ECMWF triangular–cubic–octahedral (TCo1279) operational grid at 9 km resolution, however distributed as monthly averages in a regular latitute–longitude grid (see below). Muñoz-Sabater et al. (2021) present a broad evaluation of ERA5-Land showing a median Pearson correlation of approximately 0.63 between soil moistures calculated and measured in Europe for 20 cm and 50 cm depth.

This is complemented by GLDAS, NASA's Global Land Data Assimilation System (Rodell et al. 2004), namely its Noah Land Surface Model L4 V2.1 (Beaudoing and Rodell 2020), the worst of the root-zone soil moisture products evaluated by Beck et al. (2021). Both CHTESSEL and Noah work with texture groups and use similar soil layer structures (regarding Noah cf. UCAR 2023); the quality gap to ERA5 may result from the driving reanalysis data, a coarser grid resolution or longer time steps.

In addition to mHM, ERA5, and GLDAS, we investigate the soil moisture data in the hydrological model LISFLOOD, used in V4 of the European Flood Awareness System EFAS (Mazzetti et al. 2020), and SoMo.ml-EU, an entirely observation-based soil moisture data set generated by machine learning (O et al. 2022).

Many other globally integrated SM data exist, e.g. from the U.S. Air Force Agriculture Meteorology Modeling System (Eylander et al. 2022), or from the Chinese Academy of Science's Atmosphere–Vegetation Interaction Model (AVIM; Ji 1995, Lv et al. 2021) but they are not publicly available for scientific exploitation. There are also cases in which input data and model code are provided, but not the soil moisture output. Besides individual studies (e.g. Kim et al. 2021) this affects JULES, the land model of the UK Met Office (Wiltshire et al. 2020, Gómez et al. 2020). Deliberately not considered were also data labeled "available on request" albeit this excluded the data of WAYS, a global hydrological model specifically developed for root zone water storage simulation (Mao and Liu 2019), the different HBV outputs used by Beck et al. (2021), or mHM simulations over Europe (Moravec et al. 2019, 2021).

2.2 Data and Methods

2.2.1 Weather data and SPEI calculation

The observed weather data basis used in this study were the 0.1-degree grids of E-OBS v27.0e containing daily data of several meteorological variables over Europe for the years 1950–2022 (Cornes et al. 2018, C3S 2023). We aggregated monthly values for maximum and minimum air temperature and precipitation for the years 1968–2022. Only grid cells that had complete coverage of all three variables on all days within this period were considered in this aggregation, this excludes parts of Italia, most of Greece, and large parts of Eastern Europe. An imputation method for hole-filling of E-OBS data had recently been developed at PIK, but the

application to the v27.0e data released in April 2023 was still in the making when this assessment was being compiled.

The Standardized Precipitation-Evapotranspiration Index (SPEI, Vicente-Serrano et al. 2010, Beguería et al. 2014) had been calculated from these monthly E-OBS fields using Hargreaves evapotranspiration with the SPEI software package v1.7 (Beguería and Vicente-Serrano 2017) for R (used with R version 3.6.3). We learned about the 2023 package updates to v1.8.1 too late; according to the update announcement the error in the Hargreaves calculation reported for v1.7 should however not exceed 0.1 percent. The SPEI was calculated using the standard rectangular kernel for time scales of 1, 2, 3, 4, 6, 9, 12, 18, 24, and 36 months. The original index time series of each raster cell have been rescaled from standard normal to uniform distribution on the [0,1]-interval; the original idea was to match the mHM SMI distribution (see below), and we decided to stick to uniform distributions to de-emphasize the influence of extreme values in the correlations assessment.

2.2.2 Soil moisture data and SMI calculation

We start our analyses with the soil moisture index of the UFZ Drought Monitor (UFZ 2023) calculated by the mesoscale hydrological model (mHM; Samaniego et al. 2010, Kumar et al. 2013) which is limited to Germany but considers the effects of the country's diverse soil landscapes through about 70 different soil profiles and their hydrological properties over 1.8 m depth. The mHM soil moisture index (mHM SMI) could be obtained for the years 1951–2022 in monthly time steps, however daily from 30 January 2019 on. It uses a 4-km raster based on an outdated German national map datum (DHDN zone 4, EPSG:31468). We discarded the months before 1971-01 and aggregated the daily data to monthly values from 2019-02 to 2022-12 to obtain a consistent time series of 52 years matching the availability of SPEI maps for all scales.

Soil moisture from ERA5-Land could readily be obtained in form of monthly averages for the entire 1971–2022 time range and on a regular 0.1-degree grid (Muñoz-Sabater et al. 2019). There are however separate volumetric soil moistures given in percent for three layers (0–7 cm, 7–28 cm, and 28–100 cm depth); we multiplied these by the respective layer thicknesses before summing them up to absolute water contents in mm. Spuriously occurring negative values were set to zero. For each raster cell, the time series of water contents was transformed to soil moisture indices more or less equally distributed on the [0,1]-interval using the standard density estimation of the R software.

The LISFLOOD soil moisture data (Mazzetti et al. 2020) are samples from the 15th of each month (the model operates on 6-hour time steps, and aggregations were not available). They are provided in a 5-km raster based on ETRS89 / LAEA Europe (EPSG:3035) complying with the standard grids used by European statistical offices. The calculation to obtain the LISFLOOD

SMI was practically the same as with ERA5, only the three layers had depths of 0–10 cm, 10–30 cm, and 30–50 cm, and the temporal coverage was limited to the years 1991–2022.

GLDAS-Noah is the only of the GLDAS Land models whose data are provided in 0.25 degrees resolution (Beaudoing and Rodell 2020), the other alternatives are even coarser with 1-degree grids. Noah soil moisture data are provided as absolute values for four layers, 0–10 cm, 10–40 cm, 40–100 cm, and 100–200 cm; these were simply added before our GLDAS SMI calculation took place. With the years 2000–2022 the time coverage was even shorter than for LISFLOOD. Previous years would have been available from a former model version only, and such inconsistency should be avoided.

The SoMo.ml-EU data (O et al. 2022) have the same layer configuration as LISFLOOD, 0–10 cm, 10–30 cm, and 30–50 cm, and their volumetric water contents are treated alike to obtain the SoMo SMI. The data are also provided on a regular 0.1-degree grid; the time range is however limited to 2003–2020, and it is unlikely that this demonstrator data set will ever be extended.

2.2.3 Correlation mapping

To map the Pearson correlations between the local time series of differently scaled SPEIs and the various SMIs a common raster geometry had to be chosen and necessary reprojections to be performed. For the German mHM data its original 4-km DHDN raster was used; SPEIs were regridded with bilinear interpolation. ERA5-Land and SoMo.ml-EU datasets could be practically directly applied due to their consistent 0.1-degree grid (considering only certain differences in the extent of the map rectangles). The GLDAS-Noah data in 0.25-degree resolution and the SPEI data in 0.10-degree resolution were both resampled to a common 0.05-degree grid using the nearest-neighbour principle (effectively leading to an overlap of internally homogeneous grid boxes of different sizes). For LISFLOOD, the SPEI data were bilinearly interpolated to its 5-km grid.

This ETRS89 / LAEA grid was also applied for the visualizations; it provides an equal-area projection with minimum distortion in Central Europe (projection centre at 52°N, 10°E). Consequently, the other correlation maps were also resampled to this grid using the nearest-neighbour method. Finally, two extra maps were produced for each SMI: one showing the local maxima of the correlation maps for the different SPEI scales and one showing the respective optimal scales.

2.3 Results

2.3.1 UFZ Drought Monitor / mHM

First we will look at the correlations between the UFZ Drought Monitor's Soil Moisture Index (SMI) and the 1-month SPEI. With the time scale equalling the temporal resolution of the input weather data the SPEI indicates the relative positions of the actual climatic water balances within their monthly distributions expressed in *Z* metrics, there is no extra time lag except the monthly aggregation. Given the hysteresis of the water content in most soils, higher correlations can only be expected in places with shallow or stony soils with low storage capacities and high percolation rates.

Figure 1 shows that this assumption is probably correct: Among the spatial patterns displayed there there is a boomerang-shaped structure of higher correlations in Southern Germany. An overview map of German major soil landscapes (BGR 2008) displayed in Figure 2 shows this “boomerang” in deep-pink indicating shallow soils on limestones, and the biggest respective blob matches the higher-correlation structure in Fig. 1.

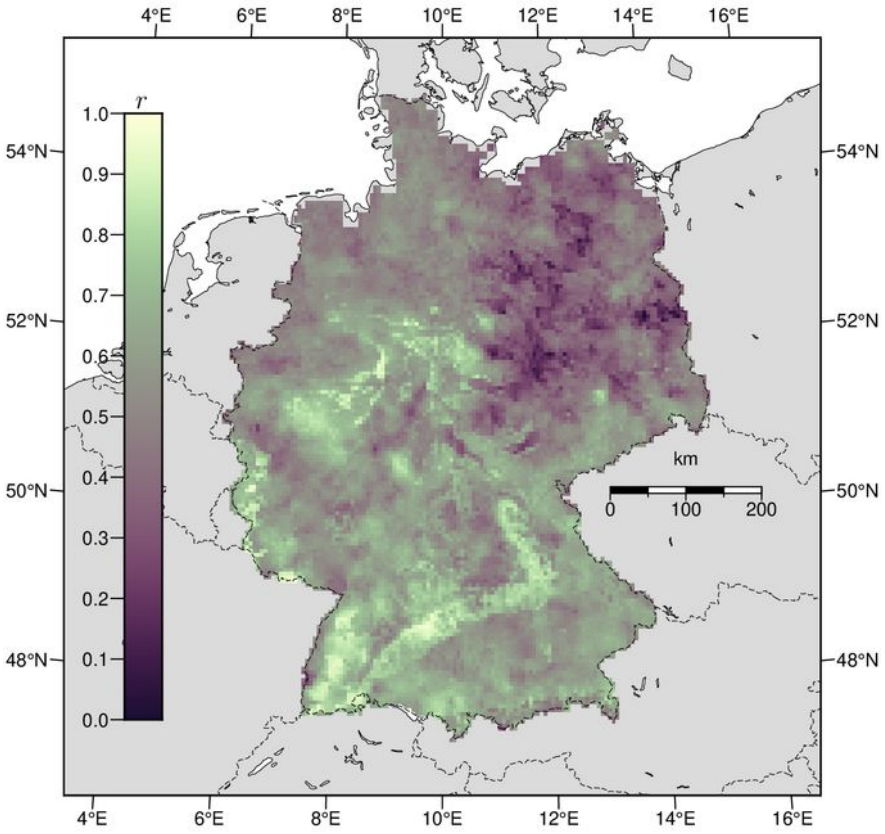

Figure 1: Map of Pearson correlations between monthly values of the Soil Moisture Index of the UFZ Drought Monitor and SPEI-1 calculated from E-OBS data.

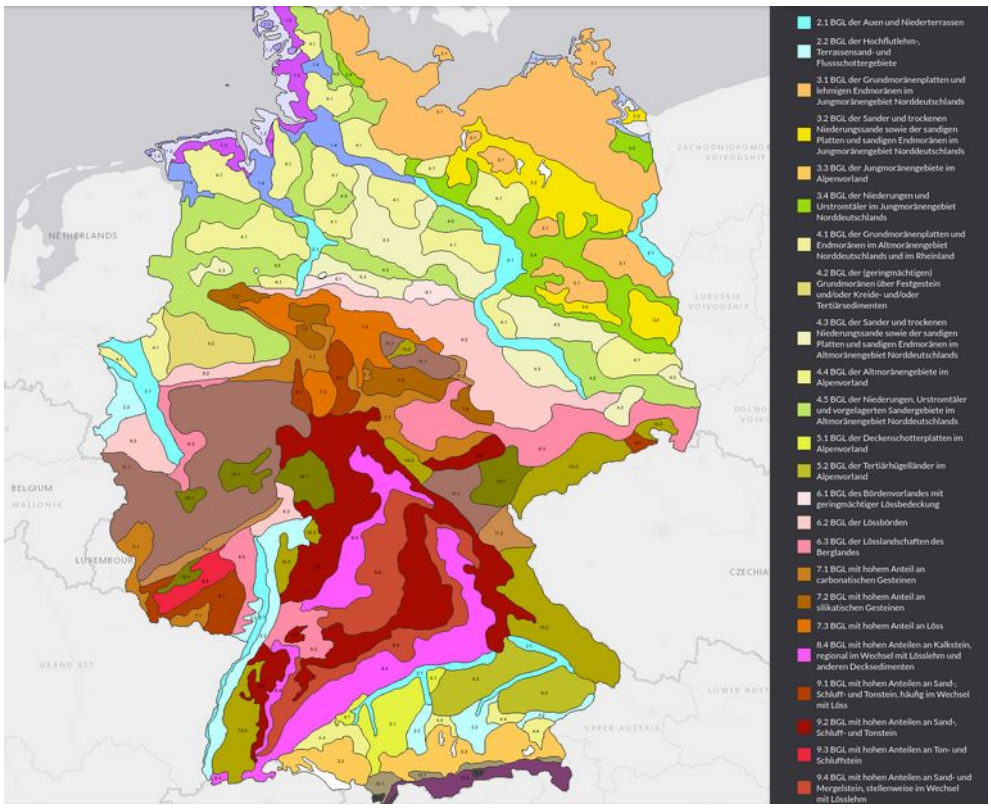

Figure 2: Map of the major German soil landscapes (Bodengroß-landschaften, BGR 2008). Screenshot from the BGR Geoviewer (https://services.bgr.de/boden/bgl5000, 2023-05-04) reproduced at approximate 1 : 8 000 000 scale in accordance with the German legislation on geodata use (GeoNutzV).

This structure resembles the German Jura highlands (German: *Alb*), namely the Swabian Jura in the west and the Franconian Jura in the east including the northward-bending wing of the "boomerang". As the English names suggest, they consist in large parts of Jurassic limestone with the respective soil-hydraulic properties. Karst is also a frequent feature in the Swabian Jura. The quick drying (and rewetting) of the Swabian Jura is also visualized in a regional soil drought assessment (Tijdeman and Menzel 2021).

Figure 3 displays the results for the longer SPEI timescales up to 36 months. As one could expect, the Jura structure appears darker than its surroundings on the longer scales, especially 9–18 months. Subfigure 4d) showing the correlations for SPEI-6 is generally the brightest map with the highest average *r*: 0.575. This recommends SPEI-6 as easy-to-calculate general drought indicator for Germany if no additional soil information should be considered. However, for the many distinct landscapes in the country individual scales are preferrable. For example, there is a high-correlation triangle appearing to the west of the map centre on the 3- and 4-months time scales. This is the Sauerland, part of the Rhenish Massif characterized by relatively high precipitation (> 1000 mm per year, the German average is about 790 mm per year) and soils formed on slate rocks. High correlations on long time scales (18–36 months) are restricted to lowland areas with deep sediments and soils, e.g. the Rhine Valley or loess areas. These have respectively long soil water turnover times.

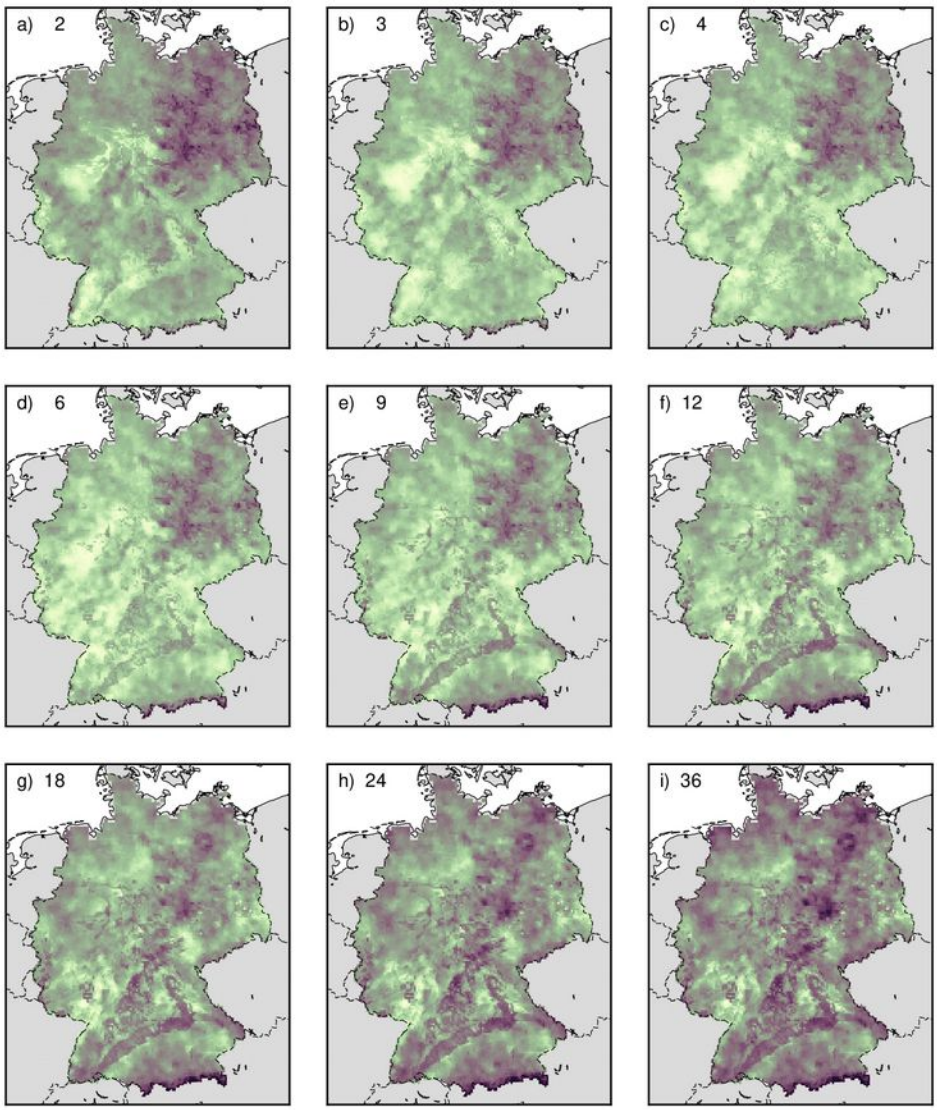

Figure 3: Pearson correlations between monthly values of the Soil Moisture Index of the UFZ Drought Monitor (mHM SMI) and SPEI on different time scales: a) 2 months, b) 3 months, c) 4 months, d) 6 months, e) 9 months, f) 12 months, g) 18 months, h) 24 months, and i) 36 months. Colour scale as in Fig. 1.

To obtain a better SPEI proxy for the SMI situation in all landscapes it seems reasonable to compose a map from SPEI values of different scales: Then each raster cell takes the SPEI of the scale that yielded the highest correlations to the SMI. The spatial distribution of optimized correlations achieved by this approach is shown in Figure 4, and Figure 5 indicates where which scale had been applied.

Correlation values of 0.6 and above are reached in 60% of the country, the average is 0.606 and the median 0.623. In some parts of Eastern Germany the soil moisture situation can however not be satisfactorily approximated by any of the SPEIs. Despite the probably nonlinear hysteresis of the soil water storage to the meteorological situation in these areas, the time scales of their best linear approximations form smooth spatial gradients to the neighbouring areas in the map in Fig. 5.

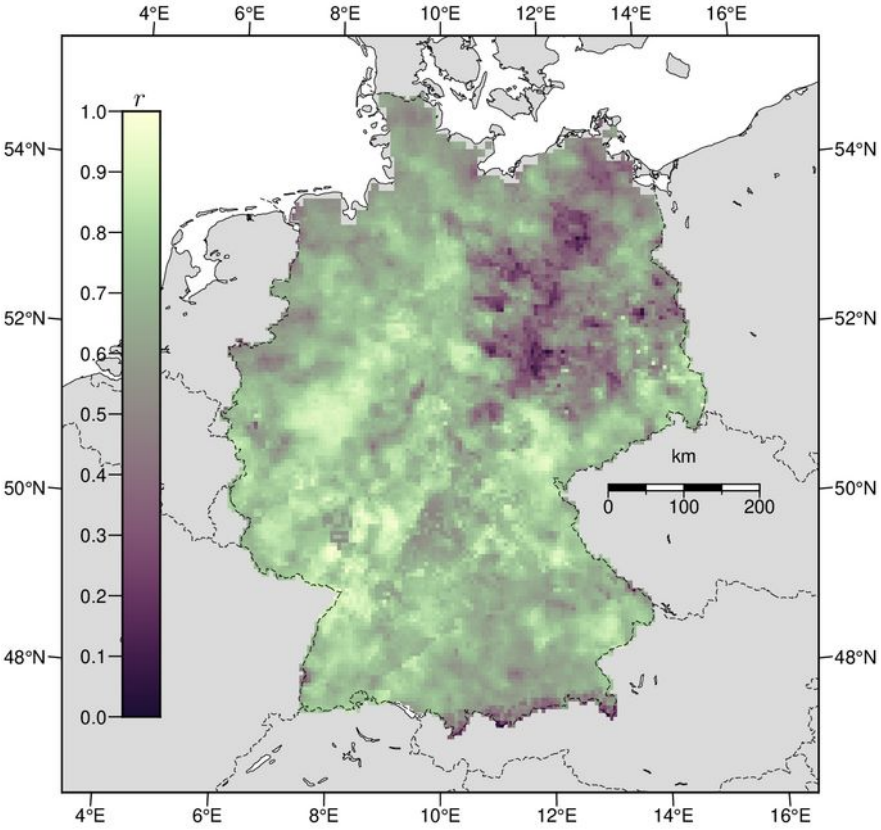

Figure 4: Maxima of the correlations between mHM SMI and SPEIs of ten different time scales ranging from 1 to 36 months.

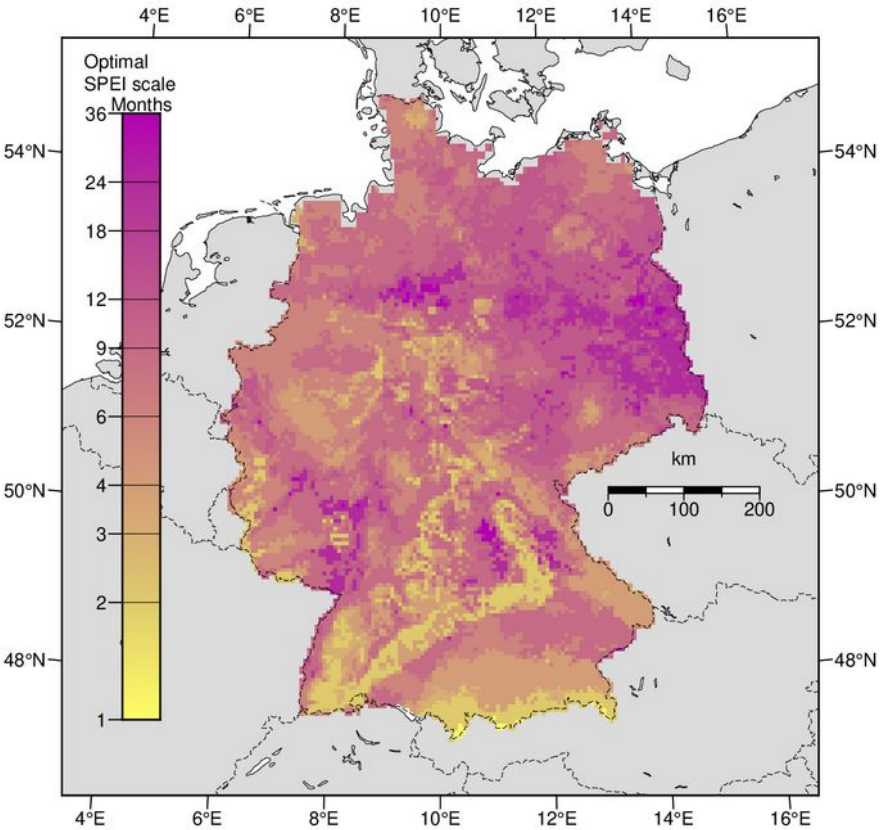

Figure 5: Spatial distribution of the SPEI time scales used for the optimal local correlations with mHM SMI depicted in Fig. 4.

We can also spot some yellow pixels in Fig. 5 indicating the 1-month SPEI timescale at the southern border. This edge cuts the northern fringes of the Alp mountains where immediate reactions can be expected due to the rocky substrates but hardly be detected from the correlation maps alone. In general, the structures in Fig. 5 appear to correspond better than any of the correlation patterns to the major soil landscapes of Fig. 2 – a clear indication that the mesoscale hydrological model (mHM) behind the UFZ Drought Monitor (UFZ 2023) appropriately considers the regionally differing hydraulic landscape properties in its soil water calculations.

2.3.2 ERA5-Land

The ERA5 model does not show the same detailed structures within Germany, but longer SPEI scales, albeit on a lower level, are also more appropriate in Eastern Germany as soil moisture status proxy (Figs 6 and 8).

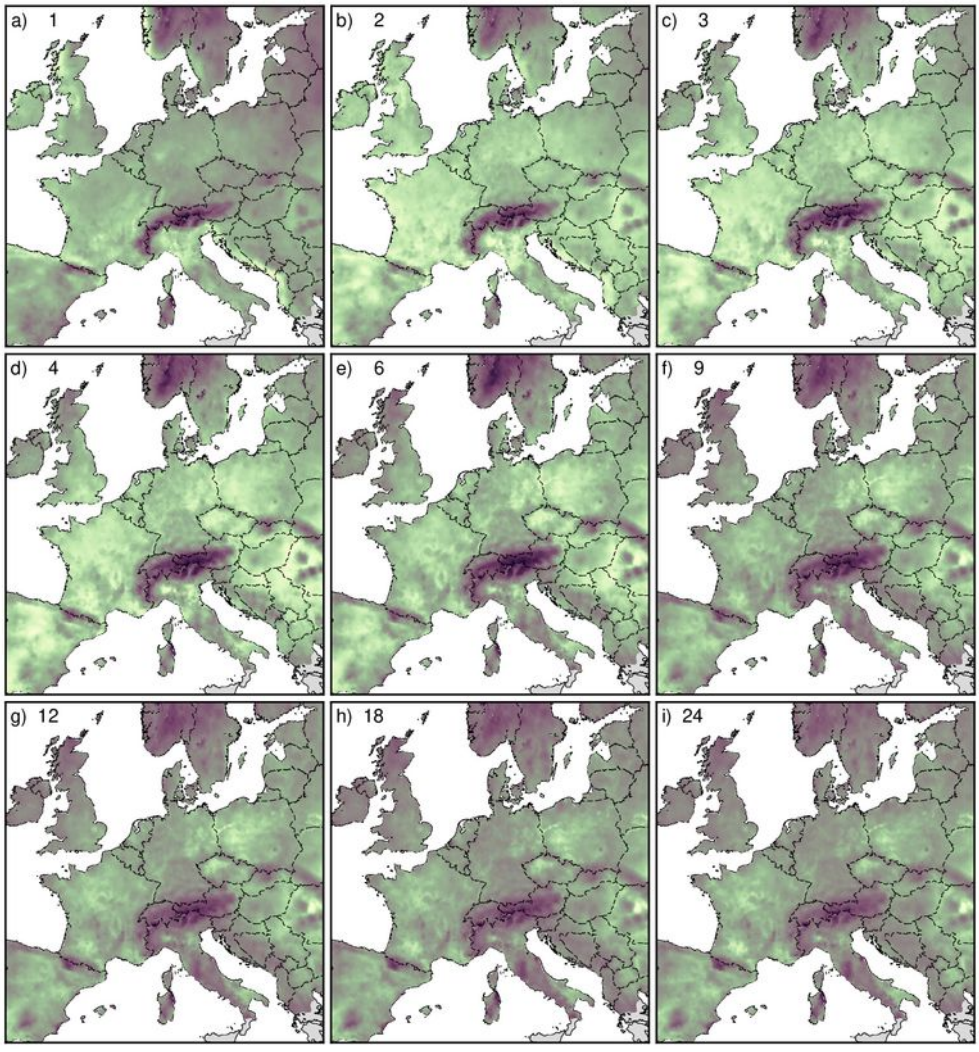

Figure 6: Pearson correlations between monthly values of the ERA5 SMI and SPEI on different time scales: a) 1 month, b) 2 months, c) 3 months, d) 4 months, e) 6 months, f) 9 months, g) 12 months, h) 18 months, and i) 24 months. Colour scale as in Fig. 7.

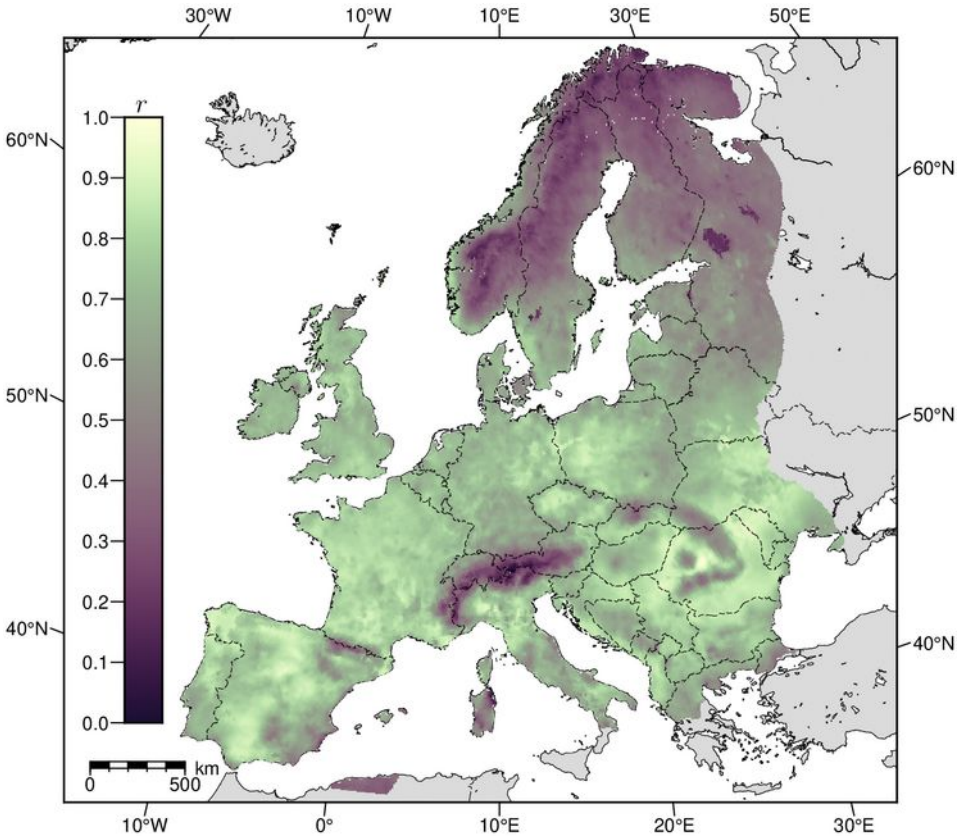

Figure 7: Maxima of the correlations between ERA5 SMI and SPEIs of ten different time scales ranging from 1 to 36 months.

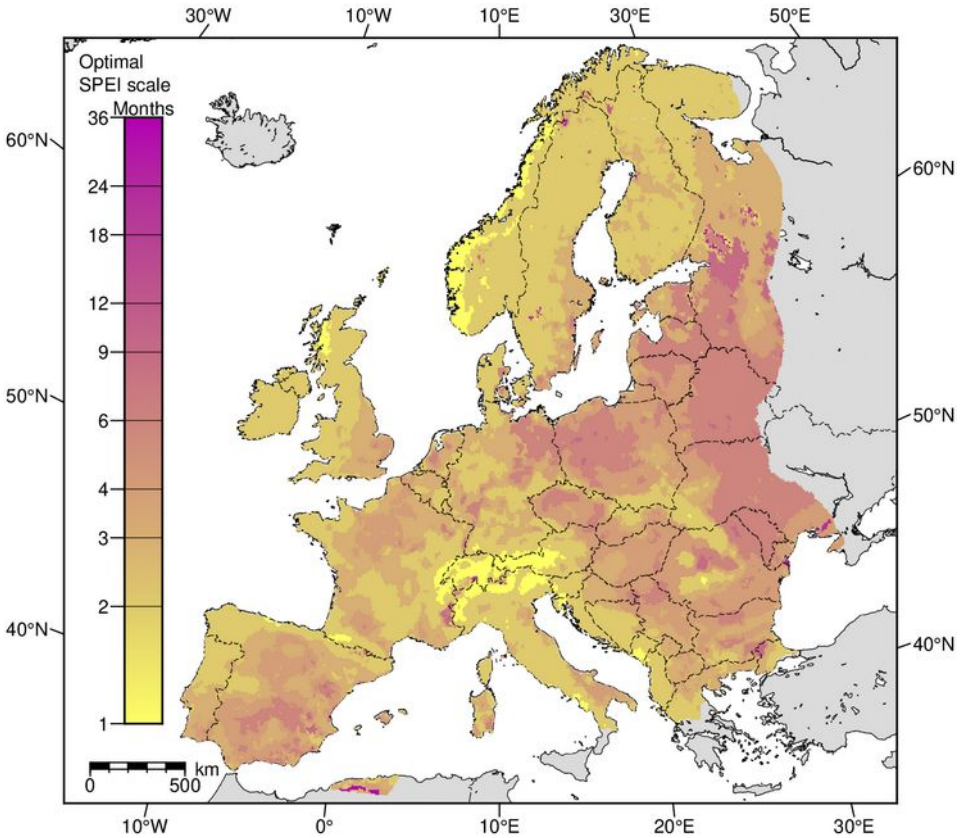

Figure 8: Spatial distribution of the SPEI time scales used for the optimal local correlations with ERA5 SMI depicted in Fig. 4.

The ERA5 map of maximum correlations (Fig. 7) has got an average of 0.490 and a median of 0.539. Especially in mountainous areas there is no simple relationship between SPEI and SMI, the prevalence of shorter scales in these regions (Fig. 8) seems however realistic.

2.3.3 LISFLOOD

The LISFLOOD correlation maps provide a scattered impression. Especially in mountainous regions there are small areas with the shortest and longest optimum time scales clashing together. Keeping in mind that LISFLOOD was set up for flood forecasting, matching observed runoff curves will probably have been the priority in model calibration, not soil moisture patterns. The patchwork of optimum time scales might then well resemble the structure of gauge catchments which received individual (and partly extreme) calibration parameters biasing the soil water budget. The average of the optimum correlations (Fig. 10) is only 0.386, and their median is 0.410.

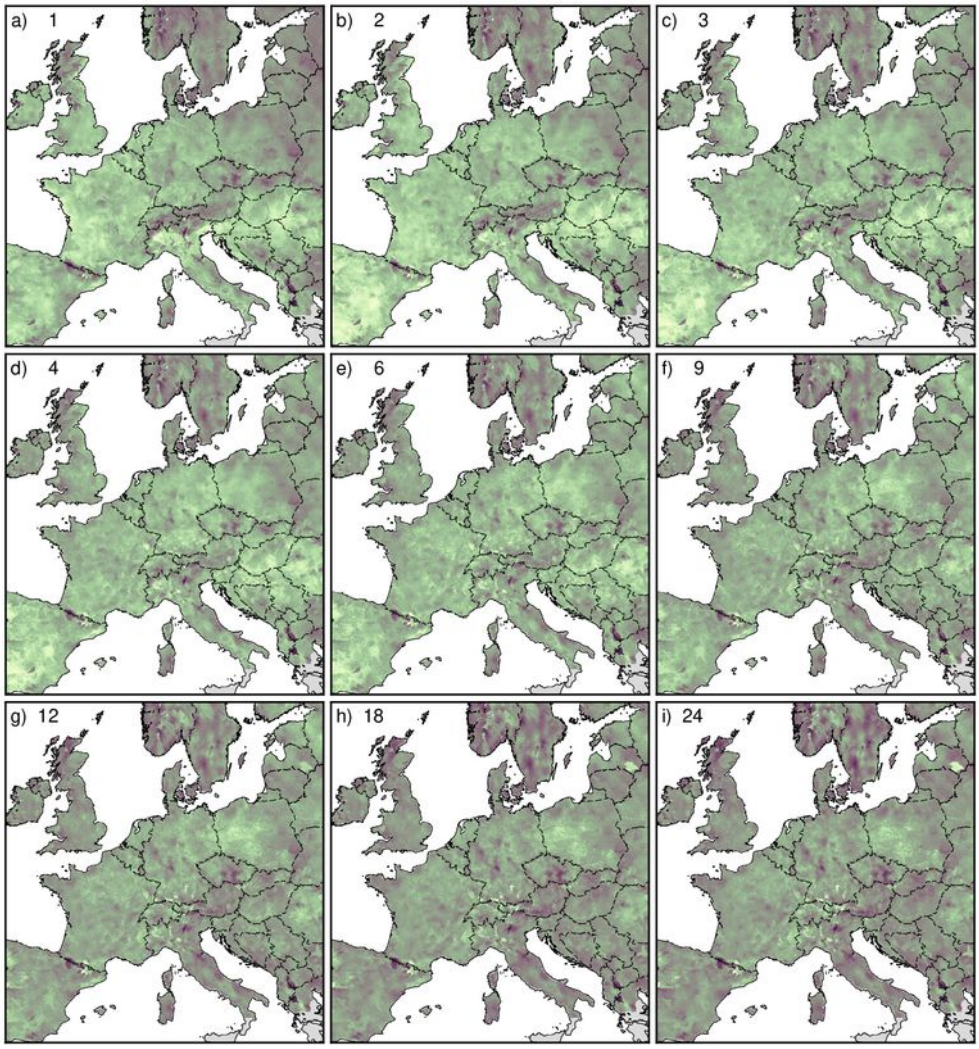

Figure 9: Pearson correlations between monthly values of the LISFLOOD SMI and SPEI on different time scales: a) 1 month, b) 2 months, c) 3 months, d) 4 months, e) 6 months, f) 9 months, g) 12 months, h) 18 months, and i) 24 months. Colour scale as in Fig. 10.

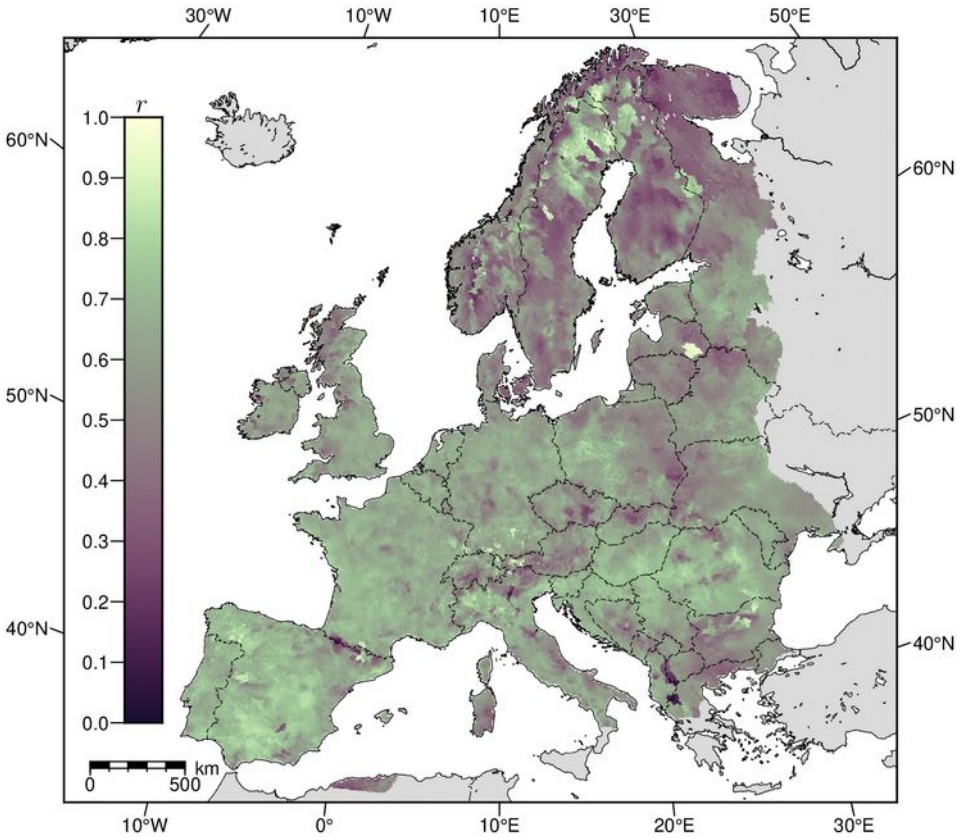

Figure 10: Maxima of the correlations between LISFLOOD SMI and SPEIs of ten different time scales ranging from 1 to 36 months.

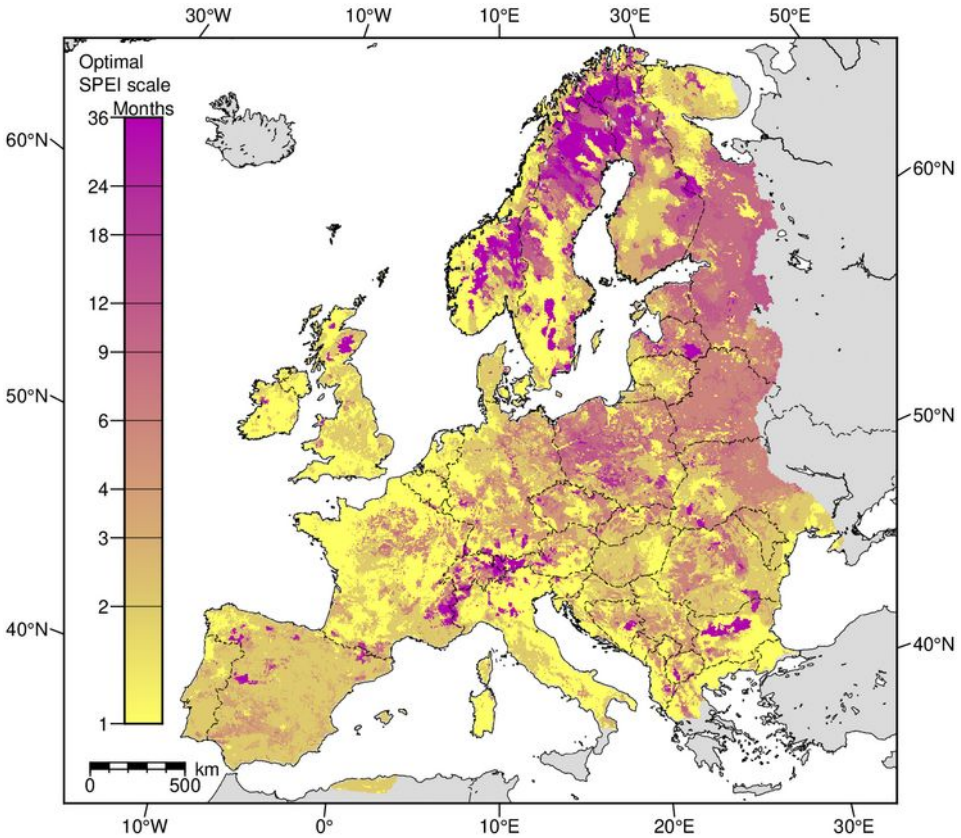

Figure 11: Spatial distribution of the SPEI time scales used for the optimal local correlations with LISFLOOD SMI depicted in Fig. 10.

2.3.4 GLDAS-Noah

The GLDAS-Noah model shows certain similarities to the ERA5-Land results with the mountain ranges exposing generally low correlations. In contrast to ERA5 there are also a lot of areas with very long optimal scales in mountainous areas, and the broader patterns in the lowlands do not match very well (Fig. 14). Part of the generally noisier appearance of the GLDAS results is however owing to the coarser input grids and the nearest neighbour resampling applied. As already mentioned, Beck et al. (2021) found ERA5 superior to GLDAS regarding the accuracy of soil moisture. Nevertheless, there are larger lowland areas reaching very high correlations with GLDAS SMI, especially in the Danube basin, and this leads to a maximum correlation (Fig. 13) average of 0.544 and a median of 0.562, a brighter image than the respective ERA5 map in Fig. 7.

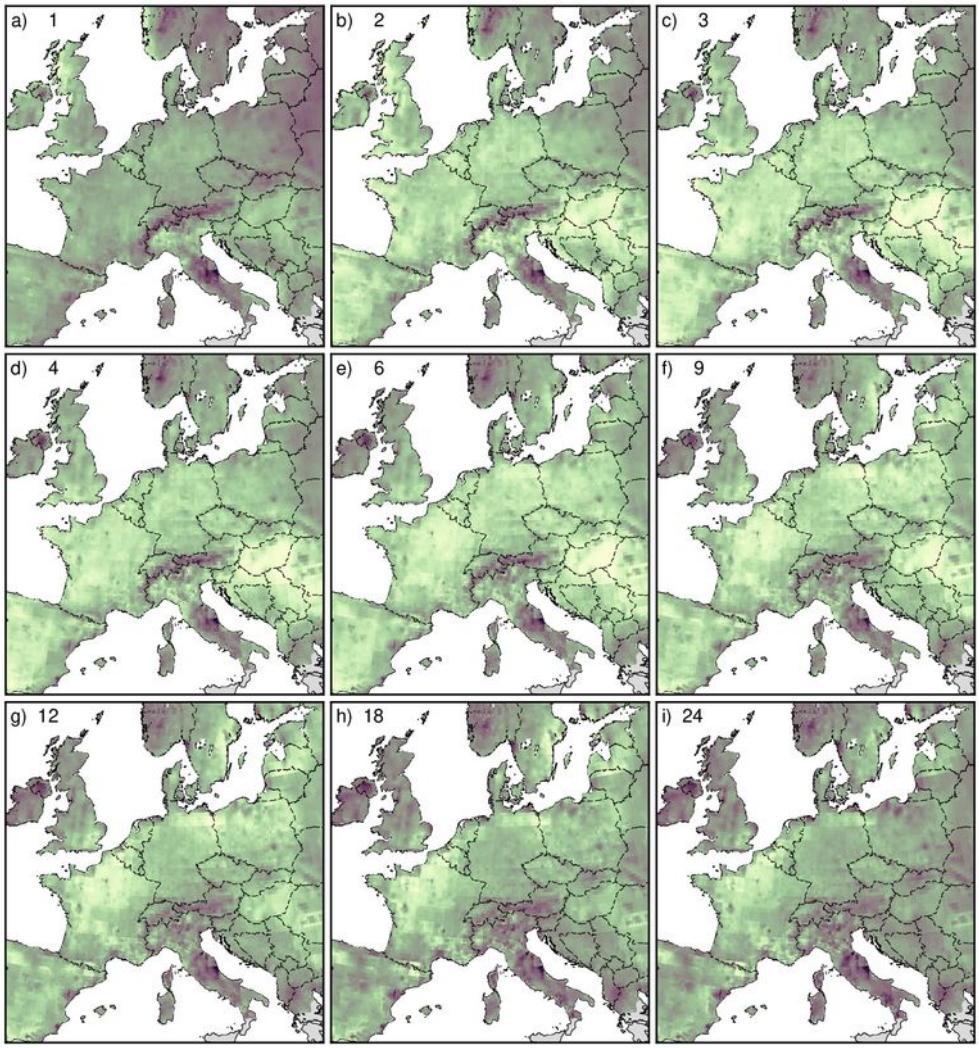

Figure 12: Pearson correlations between monthly values of the GLDAS SMI and SPEI on different time scales: a) 1 month, b) 2 months, c) 3 months, d) 4 months, e) 6 months, f) 9 months, g) 12 months, h) 18 months, and i) 24 months. Colour scale as in Fig. 13.

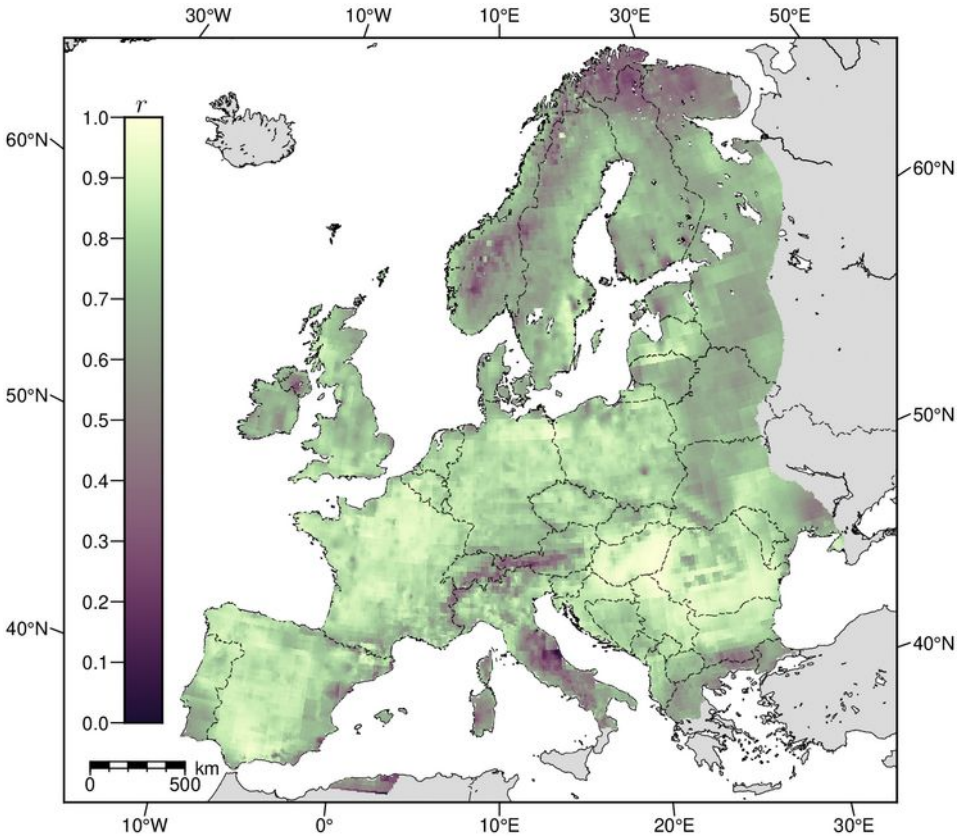

Figure 13: Maxima of the correlations between GLDAS SMI and SPEIs of ten different time scales ranging from 1 to 36 months.

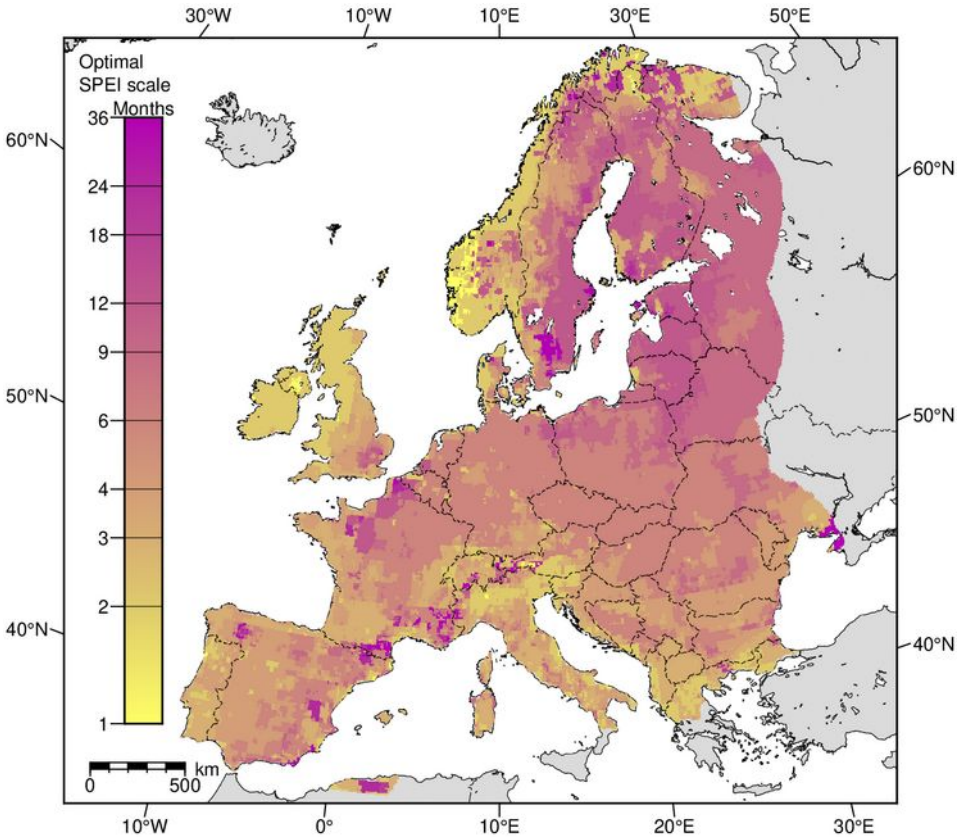

Figure 14: Spatial distribution of the SPEI time scales used for the optimal local correlations with GLDAS SMI depicted in Fig. 13.

2.3.5 SoMo.ml-EU

The field observation-based SoMo.ml-EU results expose aspects of both the ERA5 maps, especially the homogeneously short optimum SPEI scales in mountainous areas (Figs 8 and 17), and the GLDAS maps, note here a common preference for longer optimum time scales in the lowland regions around the Baltic Sea (Figs 14 and 18) and the clustering of the highest within-map correlations in the Danube basin (Figs 13 and 16). Interestingly there are only small areas in the mountainous regions with very low correlations for all SPEI scales, this relativizes the absence of high maximum correlations; the average of Fig. 16 is still at 0.539, and the median at 0.555. The German soil landscape structures (Fig. 2) can not easily be spotted in the SoMo.ml-EU results, but compared to the European model outputs there are at least some relations, note for instance the yellow for the 1-month optimum time scale on a couple of mountain ranges in Fig. 17.

Figure 15: Pearson correlations between monthly values of the SoMo.ml

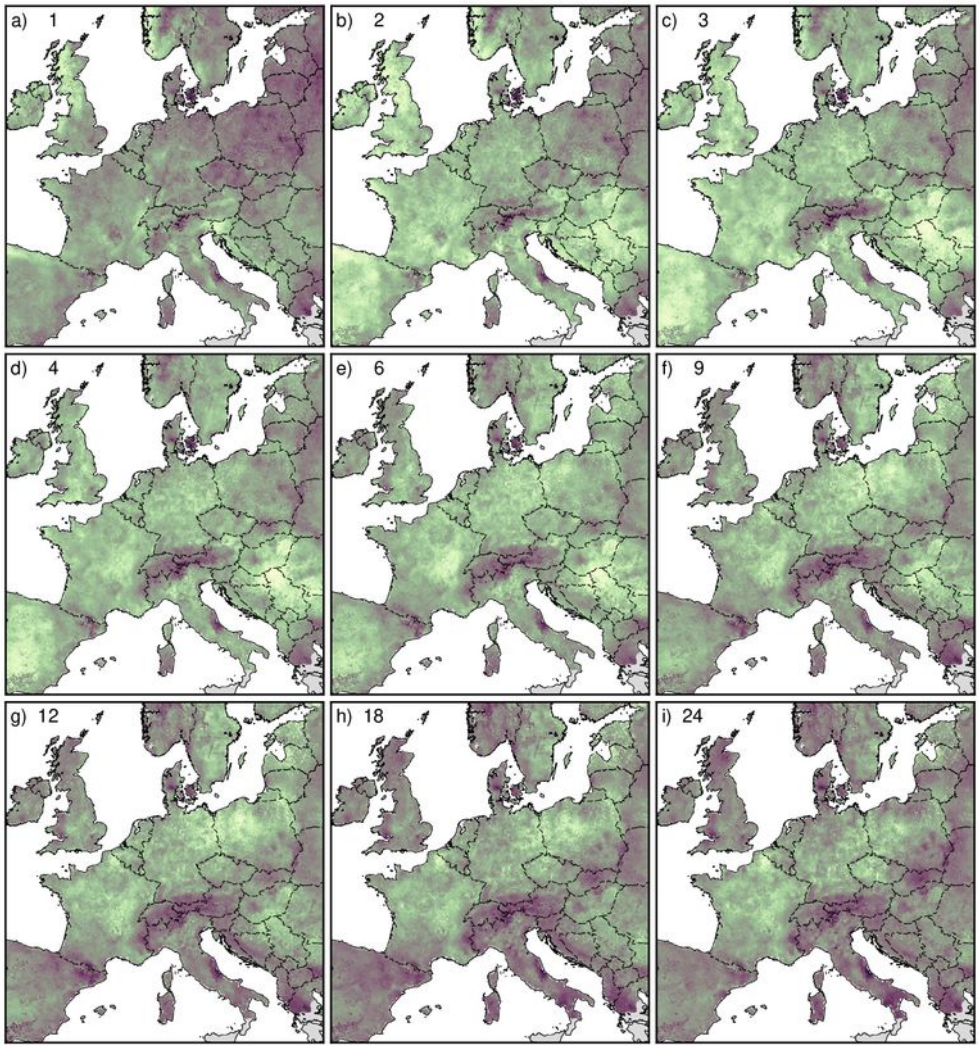

SMI and SPEI on different time scales: a) 1 month, b) 2 months, c) 3 months, d) 4 months, e) 6 months, f) 9 months, g) 12 months, h) 18 months, and i) 24 months. Colour scale as in Fig. 16.

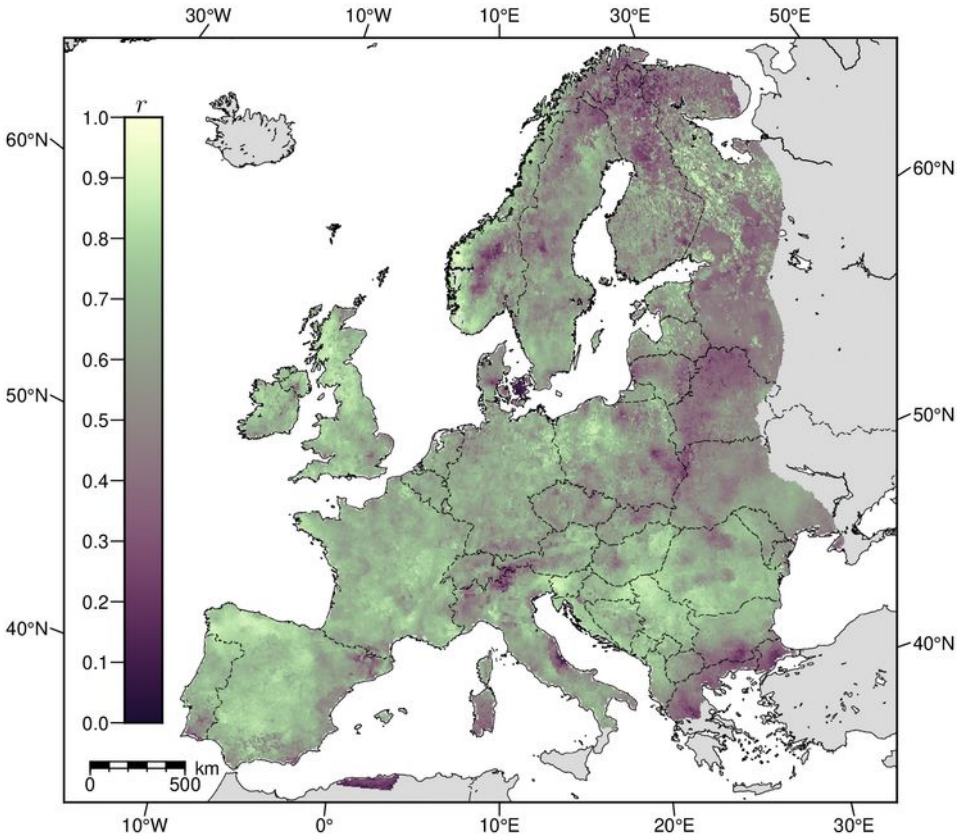

Figure 16: Maxima of the correlations between SoMo.ml-EU SMI and SPEIs of ten different time scales ranging from 1 to 36 months.

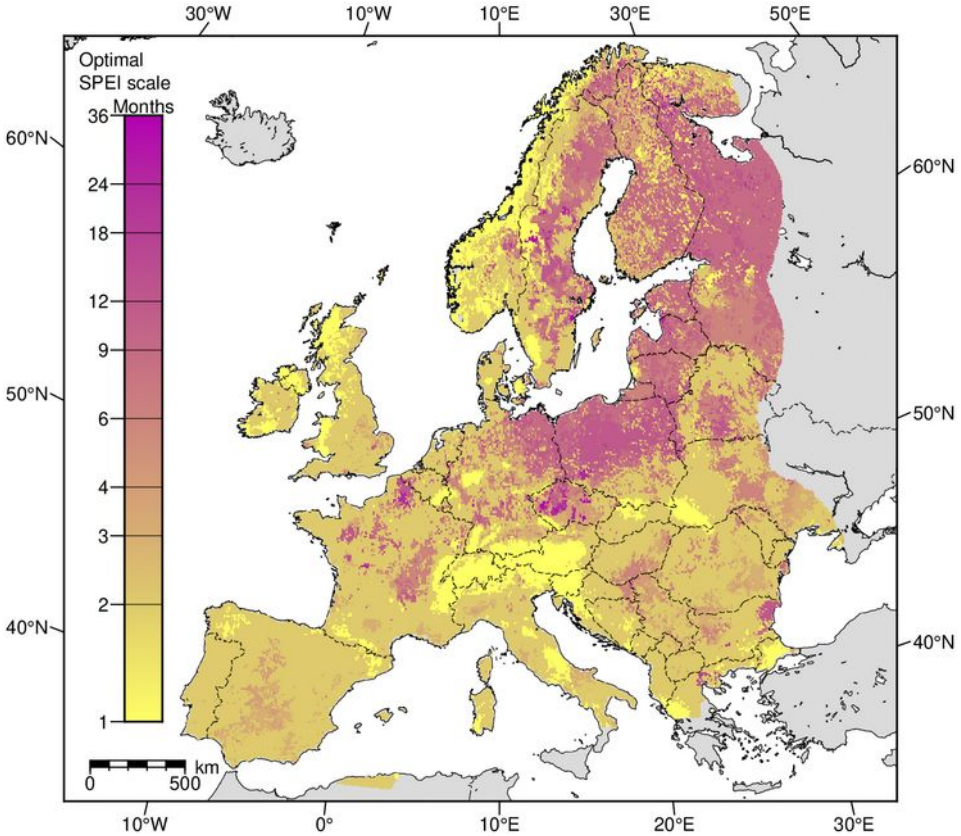

Figure 17: Spatial distribution of the SPEI time scales used for the optimal local correlations with SoMo.ml-EU SMI depicted in Fig. 16.

2.4 Discussion and Conclusion

A fundamental problem that became obvious from the wide differences between the results for the different SM products is their questionable quality on global or continental scales. Local evaluations using observed SM (e.g. Huang et al. 2022) cannot inform about the model fidelity on continental scale but show high discrepancies even between different versions of a model (Yang et al. 2022). The most probable reason for these problems are the generally very coarse and simple (mis-)representations of the soil landscapes.

Another example for largely disregarding local soil conditions in modelling soil moisture in the climate modelling community is given by Raoult et al. (2021). They fit a parameter in ORCHIDEE LSM, the land component of the French Earth System Model, to match drydown trajectories after rainfall events observed at 18 sites distributed around the world, notably with very different vegetation types and aridity conditions. From their results, the parameter does not appear correlated to soil type, and a global soil map is probably not considered at all in the French climate modelling so far. Had there been a high number of sites or only Central European agricultural plots, a correlation would have been detected very likely. Consequently, using a multitude of soil moisture measurements from space, McColl et al. (2017) did confirm the effect of the sand content for drying (albeit only for the radar-accessible top layer and with many gaps over Europe).

The issue of soil properties generally being neglected in earth system models has also been pointed out by Fatichi et al. (2020). Albeit there are some teams working on integrating this information into their modelling it will probably take a decade until we advance from lab testing to regular consideration in operational soil moisture products.

Looking at the individual correlation and optimum scale maps produced for this study, some observations have already been interpreted in the results section, namely: the frequently observed absence of higher correlations in mountainous areas where at the same time short optimum SPEI scales fit the assumption of shallow soils on rocks whose water content depends largely on the actual meteorological conditions, the patchiness of the optimum scale map for LISFLOOD (Fig. 11) as probable result of hydro-graph-only optimizing parameter calibrations in river gauge catchments, or the comparably coarse GLDAS-Noah grid and the reanalysis data used as possible reasons for the noisy appearance and deletion of smaller landscape structures.

Comparing the key characteristics of the soil moisture products covering all of Europe (Table 1) LISFLOOD drops out with exceptionally low correlations; this model follows other priorities than realistically capturing soil moisture dynamics. Among the other three data sources we can see longer SPEI scales preferred for deeper soils which makes sense because soil storage hysteresis can be expected to increase with profile depth.

Table 1: Key characteristics of the European soil moisture products

Data source	Soil depth	Median opt. *r*	Optimal scales
ERA5	1.0 m	0.539	1–4 months
LISFLOOD	0.5 m	0.410	very diverse
GLDAS-Noah	2.0 m	0.562	around 6 months
SoMo.ml-EU	0.5 m	0.555	2 mon. dominant

The UFZ mHM was not included in Table 1 because of its limited geographical focus, but with a considered soil depth of 1.8 m the appearance of many longer time scales in Fig. 5 (the geometric mean may also be close to 6 months) fits the picture.

Taking these observations together: Can the initial idea for a SPEI-based soil drought mapping be further pursued given the diverse limitations of the existing products despite their much higher computational effort? Our answer would be a cautious yes, but the originally intended route to just apply one of the optimal scale maps would not reach the target. If the best openly available soil moisture products correlate to the real world soil moisture with $r_{model} \approx 0.63$ (Muñoz-Sabater et al. 2021 for ERA5-Land over Europe; mind that the higher numbers of Beck et al. 2021 were limited to the top 5 cm layer), and the mimicking of these products by SPEIs of different scales works with $r_{SPEI} \approx 0.55$ (cf. Table 1), no better correlation between this potential SPEI product and the real world soil moisture than $r_{model} \cdot r_{SPEI} \approx 0.35$ can be expected. Before designing a SPEI approximation to the continental root-zone soil moisture there must be a reference data set of the latter derived from actual measurements as intelligently as possible.

This draws our attention to the SoMo.ml-EU data (O et al. 2022) which attempted to provide just that with the help of *machine learning*, namely long short-term memory (LSTM) modelling. A closer look in the O et al. (2022) publication and its predecessor (O. and Orth 2021 for SoMo.ml, a coarser global soil moisture data set) reveals that not all links to the "classical" reanalysis products were cut: The limited representativeness of point measurements within a grid cell was "balanced" by scaling these to the means and variabilities of the ERA5 soil moisture at the corresponding grid cells. Furthermore, some ERA5 weather data was used. Static predictors included topography, vegetation type and soil profile information from the Regridded Harmonized World Soil Data Base (HWSD) v1.2 (Wieder et al. 2014). The inclusion of HWSD data and topography (by cell means and variances of elevation) is however a clear advantage to the land model reanalyses and may explain why some smaller mountain ranges in Germany can be spotted in Fig. 17. O et al. (2022) show box plots with median correlations of approximately 0.75 to six field measurements in the 0–10 cm layer and 22 measurements in the 10–30 cm layer which were excluded from the training data.

As impressive this may read, machine learning for continuous soil moisture data is just being explored, and higher quality products can be expected in the near future. Two very recent examples for surface soil moisture are given by Skulovich and Gentine (2023) and Han et al. (2023).

Some advances are also expectable from the uptake of enhanced high-resolution *soil data with detailed profile information* such as Wise30sec (Batjes et al. 2016) and SoilGrids (Hengl et al. 2017). These were already tested for two ecohydrological models in Norwegian catchments (Huang et al. 2022). The simulated soil moisture series were evaluated but only in comparison to ERA5, GLEAM and a satellite-based product, and in all three cases only for the top layer (0–7 cm or 0–10 cm). Results were mixed with the highest correlations (0.80–0.85) observed for ERA5.

There are also developments among the reanalysis products that should be considered if our idea should be pursued further in the future: ECLand, the ECMWF Land Surface Modelling System is undergoing revision to consider orography and soil texture in runoff and infiltration parameterizations; first SM evaluations with satellite-based topsoil data were promising (Boussetta et al. 2021). This revision, introducing also additional soil layers and an experimental root distribution formulation has however not appeared in the publicly downloadable ECMWF data which still uses a static four-layer configuration of 2.89 m depth. Boussetta et al. (2021) also advertize upcoming very high resolutions of 1 km for ECLand and a generally better integration with satellite observations.

New directions for improvements by *data assimilation* have also been proposed for the Community Land Model version 5 (CLM5), the land component of the Community Earth System Model version 2 (CESM2). The global applicability of a pilot study conducted by Strebel et al. (2022) in a 38.5-ha forested catchment in Germany remains however questionable. A hybrid approach for global hydrological models combining deep learning and data assimilation was recently presented by Kraft et al. (2022). A first output data sample from their H2M model has been released (Kraft et al. 2021) but not considered for this deliverable. The H2M output is also interesting because it uses SoilGrids (Hengl et al. 2017), currently probably the best available global soil data base. A major downside is the low resolution of one degree (approx. 110 km in north–south direction).

Finally, *ensemble evaluation* should be mentioned as another strategy to obtain better predictions. The example is given by Wang et al. (2021) who developed global multilayer soil moisture data for the period 1970–2016 through ensembles of already existing data sets. As usual for ensemble data, the result performed better in comparison to field measurements than any of the input sources.

We conclude that a realistic spatio-temporal image of European soil moisture is about to emerge, and the idea of a meaningful SPEI-based soil moisture index which is easily calculated for continental scenario

projections of high resolution and with many realisations should be pursued further over the next decade.

Acknowledgments

We acknowledge the E-OBS dataset from the EU-FP6 project UERRA (http://www.uerra.eu) and the Copernicus Climate Change Service, and the data providers in the ECA&D project (https://www.ecad.eu).

References

Ajaz A, Taghvaeian S, Khand K, Gowda PH, Moorhead JE (2019) Development and Evaluation of an Agricultural Drought Index by Harnessing Soil Moisture and Weather Data. Water 11(7): 1375. https://doi.org/10.3390/w11071375

Almendra-Martín L, Martínez-Fernández J, Piles M, González-Zamora Á, Benito-Verdugo P, Gaona J (2022) Influence of atmospheric patterns on soil moisture dynamics in Europe. Sci Tot Envir 846: 157537. http://doi.org/10.1016/j.scitotenv.2022.157537

Barnard DM, Germino MJ, Bradford JB, O'Connor RC, Andrews CM, Shriver RK (2021) Are drought indices and climate data good indicators of ecologically relevant soil moisture dynamics in drylands? Ecol Indicat 133: 108379. https://doi.org/10.1016/j.ecolind.2021.108379

Batjes NH (2016) Harmonized soil property values for broad-scale modelling (WISE30sec) with estimates of global soil carbon stocks. Geoderman 269: 61–68. https://doi.org/10.1016/j.geoderma.2016.01.034

Beaudoing H, Rodell M (2020), GLDAS Noah Land Surface Model L4 monthly 0.25 x 0.25 degree V2.1. NASA/GSFC/HSL, Greenbelt, Maryland, USA; Goddard Earth Sciences Data and Information Services Center (GES DISC). Accessed on 8 May 2023. https://doi.org/10.5067/SXAVCZFAQLNO

Beck HE, Pan M, Miralles DG, Reichle RH, Dorigo WA et al. (2021) Evaluation of 18 satellite- and model-based soil moisture products using in situ measurements form 826 sensors. Hydrol Earth Syst Sci 25(1): 17–40. https://doi.org/10.5194/hess-25-17-2021

Beguería S, Vicente-Serrano SM, Reig F, Latorre B (2014) Standardized precipitation evapotranspiration index (SPEI) revisited: parameter fitting, evapotranspiration models, tools, datasets and drought monitoring. Internat J Climatol 34(10): 3001–3023. https://doi.org/10.1002/joc.3887

Beguería S, Vicente-Serrano SM (2017). SPEI: Calculation of the Standardised Precipitation-Evapotranspiration Index. R package version 1.7. https://CRAN.R-project.org/package=SPEI

Bergström S (1976) Development and application of a conceptual runoff model for Scandinavian catchments. SMHI Report RHO 7. Swedish Meteorological and Hydrological Institute (SMHI), Norrköping, Sweden, (8)+vi+134(+5) pp. http://urn.kb.se/resolve?urn=urn:nbn:se:smhi:diva-5738

Bergström S (1992) The HBV model – its structure and applications. SMHI Report RH 4. Swedish Meteorological and Hydrological Institute (SMHI), Norrköping, Sweden, 35 pp. https://www.smhi.se/en/publications/the-hbv-model-its-structure-and-applications-1.83591 – Last accessed in March 2023.

BGR (2008) Bodengroßlandschaften von Deutschland 1 : 5 000 000 (BGL5000), Version 2.0. Map of the main soil landscapes of Germany, single sheet PDF file, in German. Bundesanstalt für Geowissenschaften und Rohstoffe (BGR) [Federal Institute for Geosciences and Natural Resources], Hannover, Germany. https://www.bgr.bund.de/DE/Themen/Boden/Produkte/Karten/Downloads/BGL5000.pdf?__blob=publicationFile&v=3 – Last accessed in May 2023.

Boeing F, Rakovec O, Kumar R, Samaniego L, Schrön M et al. (2022) High-resolution drought simulations and comparison to soil moisture observations in Germany. Hydrol Earth Syst Sci 26(19): 5137–5161. https://doi.org/10.5194/hess-26-5137-2022

Bogena HR, Schrön M, Jakobi J, Ney P, Zacharias S et al. (2022) COSMOS-Europe: a European network of cosmic-ray neutron soil moisture sensors. Earth Syst Sci Data 14(3): 1125–1151. https://doi.org/10.5194/essd-14-1125-2022

Boussetta S, Balsamo G, Arduini G, Dutra E, McNorton J et al. (2021) ECLand: The ECMWF Land Surface Modelling System. Atmosphere 12(6): 723. https://doi.org/10.3390/atmos12060723

Caretta MA, Mukherji A, Arfanuzzaman M, Betts RA, Gelfan A, Hirabayashi Y, Lissner TK, Liu J, Lopez Gunn E, Morgan R, Mwanga S, Supratid S (2022) Water. In: Pörtner H-O, Roberts DC, Tignor M, Poloczanska ES, Mintenbeck K, Alegría A, Craig M, Langsdorf S, Löschke S, Möller V, Okem A, Rama B (eds) Climate Change 2022: Impacts, Adaptation and Vulnerability. Contribution of Working Group II to the Sixth Assessment Report of the Intergovernmental Panel on Climate Change. Cambridge, UK and New York, NY, USA, pp. 551–571.

Cook BI, Mankin JS, Marvel K, Williams AP, Smerdon JE, Anchukaitis KJ (2020) Twenty-First Century Drought Projections in the CMIP6 Forcing Scenarios. Earth's Future 8(6): e2019EF001461. https://doi.org/10.1029/2019EF001461

C3S (2023) E-OBS v27.0e data sets. Copernicus Climate Change Service (C3S), implemented by the European Centre for Medium-Range Weather Forecasts (ECMWF), Reading, UK. https://surfobs.climate.copernicus.eu/dataaccess/access_eobs.php#datafiles – Accessed on 28 April 2023.

Cornes R, van der Schrier G, van den Besselaar EJM, Jones PD (2018) An Ensemble Version of the E-OBS Temperature and Precipitation Datasets. J Geophys Res Atmos 123(17): 9391–9409. https://doi.org/10.1029/2017JD028200

Dai A (2011) Characteristics and trends in various forms of the Palmer Drought Severity Index during 1900–2008. Clim Dynam 116(D12): D12115. https://doi.org/10.1029/2010JD015541

Dai A (2021) Hydroclimatic trends during 1950–2018 over global land. Clim Dynam 56(11–12): 4027–4049. https://doi.org/10.1007/s00382-021-05684-1

Dorigo W, Himmelbauer I, Aberer D, Schremmer L, Petrakovic I et al. (2021) The International Soil Moisture Network: serving Earth system science for over a decade. Hydrol Earth Syst Sci 25(11): 5749–5804. https://doi.org/10.5194/hess-25-5749-2021

Eylander J, Kumar S, Peters-Lidard C, Lewiston T, Franks C, Wegiel J (2022) History and Development of the USAF Agriculture Meteorology Modeling System and Resulting USAF–NASA Strategic Partnership. Weather Forecast 37(12): 2293–2312. https://doi.org/10.1175/WAF-D-22-0064.1

Fatichi S, Or D, Walko R, Vereecken H, Young MH et al. (2020) Soil structure is an important omission in Earth System Models. Nature Comm 11: 522. https://doi.org/10.1038/s41467-020-14411-z

Gómez B, Charlton-Pérez CL, Lewis H, Candy B (2020) The Met Office Operational Soil Moisture Analysis System. Remote Sens 12(22): 3691. https://doi.org/10.3390/rs12223691

Han Q, Zeng Y, Zhang L, Wang C, Prikaziuk E, Niu Z, Su B (2023) Global long term daily 1 km surface soil moisture dataset with physics informed machine learning. Sci Data 10: 101. https://doi.org/10.1038/s41597-023-02011-7

Hengl T, Mendes de Jesus J, Heuvelink GBM, Ruiperez Gonzalez M, Kilibarda M et al. (2017) SoilGrids250m: Global gridded soil information based on machine learning. PLOS One 12(2): e0169748. https://doi.org/10.1371/journal.pone.0169748

Huang S, Eisner S, Haddeland I, Mengistu ZT (2022) Evaluation of two new-generation global soil databases for macro-scale hydrological modelling in Norway. J Hydrol 610: 127895. https://doi.org/10.1016/j.jhydrol.2022.127895

Ji J (1995) A climate–vegetation interaction model: simulating physical and biological processes at the surface. J Biogeogr 22(2–3): 445–451. https://doi.org/10.2307/2845941

Joo J, Jeong S, Zheng C, Park C-E, Park H, Kim H (2020) Emergence of significant soil moisture depletion in the near future. Envir Res Lett 15(12): 124048. https://doi.org/10.1088/1748-9326/abc6d2

Kim H, Lakshmi V, Kwon Y, Kumar SV (2021) First attempt of global-scale assimilation of subdaily scale soil moisture estimates from CYGNSS and SMAP into a land surface model. Environ Res Lett 16(7): 074041. https://doi.org/10.1088/1748-9326/ac0ddf

Kraft B, Jung M, Körner M, Koirala S, Reichstein M (2021) Daily hydrological simulation – Towards hybrid modeling of the global hydrological cycle. Data set, version 1.0. Edmond, 30 GB. https://doi.org/10.17617/3.65

Kraft B, Jung M, Körner M, Koirala S, Reichstein M (2022) Towards hybrid modeling of the global hydrological cycle. Hydrol Earth Syst Sci 26(6): 1579–1614. https://doi.org/10.5194/hess-26-1579-2022

Krysanova V, Müller-Wohlfeil D-I, Becker A (1998) Development and test of a spatially distributed hydrological/water quality model for mesoscale watersheds. Ecol Model 106(2–3): 261–289. https://doi.org/10.1016/S0304-3800(97)00204-4

Krysanova V, Hattermann F, Huang S, Hesse C, Vetter T, Liersch S, Koch H, Kundzewicz ZW (2015) Modelling climate and land-use change impacts with SWIM: lessons learnt from multiple applications. Hydrol Sci J 60(4): 606–635. https://doi.org/10.1080/02626667.2014.925560

Kumar R, Samaniego L, Attinger S (2013) Implications of distributed hydrologic model parameterization on water fluxes at multiple scales and locations. Water Resour Res 49(1): 360–379. https://doi.org/10.1029/2012WR012195.

Le T, Bae D-H (2022) Causal Impacts of El Niño–Southern Oscillation on Global Soil Moisture Over the Period 2015–2100. Earth's Future 10(3): e2021EF002522. https://doi.org/10.1029/2021EF002522

Li J, Miao C, Zhang G, Fang Y-H, Shangguan W, Niu G-Y (2021) Global Evaluation of the Noah-MP Land Surface Model and Suggestions for Selecting Parameterization Schemes. JGR Atmospheres 127(5): e2021JD035753. https://doi.org/10.1029/2021JD035753

Liu Y, Yang Y (2022) Advances in the Quality of Global Soil Moisture Products: A Review. Remote Sens 14(15): 3741. https://doi.org/10.3390/rs14153741

Lv M, Xu Z, Lv M (2021) Evaluating Hydrological Processes of the Atmosphere–Vegetation Interaction Model and MERRA-2 at Global Scale. Atmosphere 12(1): 16. https://doi.org/10.3390/atmos12010016

Mao G, Liu J (2019) WAYS v1: a hydrological model for root zone water storage simulation on a global scale. Geosci Model Dev 12(12): 5267–5289. https://doi.org/10.5194/gmd-12-5267-2019

Mazzetti C, Decremer D, Barnard C, Blick M, Carton de Wiart C, Wetterhall F, Prudhomme C (2020) River discharge and related historical data from the European Flood Awareness System, v4.0. Copernicus Climate Change Service (C3S) Climate Data Store (CDS). Accessed on 8 March 2023. https://doi.org/10.24381/cds.e3458969

McColl KA, Wang W, Peng B, Akbar R, Short Gianotti DJ et al. (2017) Global characterization of surface soil moisture dynamics. Geophys Res Lett 44(8): 3682–3690. https://doi.org/10.1002/2017GL072819

Moravec V, Markonis Y, Rakovec O, Kumar R, Hanel M (2019) A 250-Year European Drought Inventory Derived From Ensemble Hydrologic Modeling. Geophys Res Lett 46(11): 5909–5917. https://doi.org/10.1029/2019GL082783

Moravec V, Markonis Y, Rakovec O, Svoboda M, Trnka M, Kumar R, Hanel M (2021) Europe under multi-year droughts: how severe was the 2014–2018 drought period? Environ Res Lett 16(3): 034062. https://doi.org/10.1088/1748-9326/abe828

Muñoz Sabater J (2019) ERA5-Land monthly averaged data from 1950 to present. Copernicus Climate Change Service (C3S) Climate Data Store (CDS). European Centre for Medium-Range Weather Forecasts (ECMWF), Reading, UK. https://doi.org/10.24381/cds.68d2bb30 – Accessed on 17 March 2023.

Muñoz-Sabater J, Dutra E, Agustí-Panareda A, Albergel C, Arduini G et al. (2021) ERA5-Land: a state-of-the-art global reanalysis dataset for land applications. Earth Syst Sci Data 13(9): 4349–4383. https://doi.org/10.5194/essd-13-4349-2021

O. S, Orth R (2021) Global soil moisture data derived through machine learning trained with in-situ measurements. Sci Data 8: 170. https://doi.org/10.1038/s41597-021-00964-1

O S, Orth R, Weber U, Park SK (2022) High-resolution European daily soil moisture derived with machine learning (2003–2020). Sci Data 9: 701. https://doi.org/10.1038/s41597-022-01785-6

Palmer WC (1965) Meteorological drought. U.S. Weather Bureau Research Paper 45. U.S. Department of Commerce, Washington, D.C., 58pp. https://www.ncei.noaa.gov/monitoring-content/temp-and-precip/drought/docs/palmer.pdf – Last accessed in March 2023.

Qiao L, Zuo Z, Xiao D (2022) Evaluation of Soil Moisture in CMIP6 Simulations. J Climate 35(2): 779–800. https://doi.org/10.1175/JCLI-D-20-0827.1

Raoult N, Ottlé C, Peylin P, Bastrikov V, Maugis P (2021) Evaluating and Optimizing Surface Soil Moisture Drydowns in the ORCHIDEE Land Surface Model at In Situ Locations. J Hydrometeorol 22(4): 1025–1043. https://doi.org/10.1175/JHM-D-20-0115.1

Rodell M, Houser PR, Jambor U, Gottschalck J, Mitchell K et al. (2004) The Global Land Data Assimilation System. Bull Amer Meteor Soc 85(3): 381–394. https://doi.org/10.1175/BAMS-85-3-381

Samaniego L, Kumar R, Attinger S (2010) Multiscale parameter regionalization of a grid-based hydrologic model at the mesoscale. Water Resour Res 46(5): W05523. https://doi.org/10.1029/2008WR007327.

Seibert J, Bergström S (2022) A retrospective on hydrological catchment modelling based on half a century with the HBV model. Hydrol Earth Syst Sci 26(5): 1371–1388. https://doi.org/10.5194/hess-26-1371-2022

Skulovich O, Gentine P (2023) A Long-term Consistent Artificial Intelligence and Remote Sensing-based Soil Moisture Dataset. Sci Data 10: 154. https://doi.org/10.1038/s41597-023-02053-x

Strebel L, Bogena HR, Vereecken H, Hendricks Franssen H-J (2022) Coupling the Community Land Model version 5.0 to the parallel data assimilation framework PDAF: description and applications. Geosci Model Dev 15(2): 395–411. https://doi.org/10.5194/gmd-15-395-2022

Sutanto SJ, Vitolo C, Di Napoli C, D'Andrea M, Van Lanen HAJ (2020) Heatwaves, droughts, and fires: Exploring compound and cascading dry hazards at the pan-European scale. Environ Int 134: 105276. https://doi.org/10.1016/j.envint.2019.105276

Tijdeman E, Menzel L (2021) The development and persistence of soil moisture stress during drought across southwestern Germany. Hydrol Earth Syst Sci 25(4): 2009–2025. https://doi.org/10.5194/hess-25-2009-2021

UCAR (2023) Unified Noah LSM. Webpage with links to further sources. NCAR Research Applications Laboratory, University Corporation for Atmospheric Research, Boulder, Colorado, USA. https://ral.ucar.edu/solutions/products/unified-wrf-noah-lsm – Accessed in May 2023.

UFZ (2023) Drought Monitor Germany. Landing page with data resources. Helmholtz Centre for Environmental Research (UFZ), Leipzig. https://www.ufz.de/index.php?en=37937 – Last accessed in May 2023. The SMI used in this study was downloaded and extracted from https://files.ufz.de/~drought/SMI_Gesamtboden_monatlich.nc in April 2023.

Vicente-Serrano SM, Beguería S, López-Moreno JI (2010) A Multi-scalar drought index sensitive to global warming: The Standardized Precipitation Evapotranspiration Index – SPEI. Journal of Climate 23(7): 1696–1718, https://doi.org/10.1175/2009JCLI2909.1

Vicente-Serrano SM, Peña-Angulo D, Beguería S, Domínguez-Castro F, Tomás-Burguera M et al. (2022) Global drought trends and future projections. Phil Trans R Soc A 380(2238): 20210285. https://doi.org/10.1098/rsta.2021.0285

Wang Y, Mao J, Jin M, Hoffman FM, Shi X, Wullschleger SD, Dai Y (2021) Development of observation-based global multilayer soil moisture products for 1970 to 2016. Earth Syst Sci Data 13(9): 4385–4405. https://doi.org/10.5194/essd-13-4385-2021

Wells N, Goddard S, Hayes MJ (2004) A Self-Calibrating Palmer Drought Severity Index. J Clim 17(12): 2335–2351.
https://doi.org/10.1175/1520-0442(2004)017<2335:ASPDSI>2.0.CO;2

Wieder WR, Boehnert J, Bonan GB, Langseth M (2014) Regridded Harmonized World Soil Database v1.2. Data set. Available on-line [http://daac.ornl.gov] from Oak Ridge National Laboratory Distributed Active Archive Center, Oak Ridge, Tennessee, USA. http://dx.doi.org/10.3334/ORNLDAAC/1247

Wiltshire AJ, Duran Rojas MC, Edwards JM, Gedney N, Harper AB et al. (2020) JULES-GL7: the Global Land configuration of the Joint UK Land Environment Simulator version 7.0 and 7.2. Geosci Model Dev 13(2): 483–505. https://doi.org/10.5194/gmd-13-483-2020

Woodhouse CA, Pederson GT, Morino K, McAfee SA, McCabe GJ (2016) Increasing influence of air temperature on upper Colorado River streamflow. Geophys Res Lett 43(5): 2174–2181. https://doi.org/10.1002/2015GL067613

Yang S, Zeng J, Fan W, Cui Y (2022) Evaluating Root-Zone Soil Moisture Products from GLEAM, GLDAS, and ERA5 Based on In Situ Observations and Triple Collocation Method

over the Tibetan Plateau. J Hydrometeorol 23(12): 1861–1878. https://doi.org/10.1175/JHM-D-22-0016.1

Zeng J, Li J, Lu X, Wei Z, Shangguan W, Zhang S, Dai Y, Zhang S (2022) Assessment of global meteorological, hydrological and agricultural drought under future warming based on CMIP6. Atmospheric and Oceanic Science Letters 15(1): 100143. https://doi.org/10.1016/j.aosl.2021.100143

Zhao T, Dai A (2015) The Magnitude and Causes of Global Drought Changes in the Twenty-First Century under a Low-Moderate Emissions Scenario. J Clim 28(11): 4490–4512. https://doi.org/10.1175/JCLI-D-14-00363.1

Zhao T, Dai A (2022) CMIP6 Model-Projected Hydroclimatic and Drought Changes and Their Causes in the Twenty-First Century. J Clim 35(3): 897–921. https://doi.org/10.1175/JCLI-D-21-0442.1